# Pattern development in cellular automata triggered by site-specific reactive processes: Dynamical aspects

Roberto A. Garza-López and John J. Kozak*
*Department of Chemistry, Franklin College of Arts and Sciences, University of Georgia, Athens, Georgia 30602*
(Received 3 October 1988)

In this paper we continue our study of the (discretized) evolution of regular and fractal patterns initiated by a site-specific reactive event. By formulating and solving (numerically) the stochastic master equation descriptive of the model introduced (for two classes of initial conditions and for two locations of the target site), we are able to demonstrate that symmetry-breaking instabilities which generate fractal patterns (here the Sierpinski gasket) propagate slower than those which generate Euclidean ones (here the triangular lattice). A connection is made between (two) characteristics of the system's evolution (the zero-mode relaxation time and an effective relaxation time descriptive of the overall decay of the initial state) and results calculated using the theory of finite Markov processes (the mean walk length of a coreactant diffusing on the underlying lattice). Using this relationship, the trends observed in our study are interpreted in light of recent theoretical work on the problem of diffusion on fractal lattices and in terms of the notion of a "fractal" valency, a concept that places stress on insights drawn from earlier analytic and numerical studies of random processes on finite planar lattice of integral dimension $d=2$. Finally, the possible relevance of our results to a specific problem in pattern formation and development, the generation of neural networks of the Purkinje type, is discussed.

## I. INTRODUCTION

It is known from the work of Gefen, Aharony, and Alexander[1] that diffusion on percolation networks is slower than on Euclidean ones, viz., the mean-square displacement of a random walker is given by $\langle r^2(t)\rangle \sim t^{2/(2+\theta)}$ with $\theta=0.8$ in dimension $d=2$ for percolating networks versus $\theta=0$ in the Euclidean limit. To explore some consequences of this result as it relates to ongoing studies of pattern formation and pattern development,[2] we recently introduced a simple model[3] whose elaboration we hoped would cast light on this problem. The model was phrased using the language of cellular automata since, as Wolfram[4] has documented, both regular and fractal patterns[5] can be generated using simple rules in which the evolution of a given site is determined by the state values of its nearest neighbors. For example, given the eight possible states of three adjacent sites (111, 110, 101, 100, 011, 010, 001, and 000) evolving via "rule 90" (the binary code for the number 90: 01011010) a Sierpinski gasket is generated (Fig. 1), whereas "rule 50" (binary code 00110010) generates a regular triangular lattice.

In our model,[3] we considered diffusion-controlled processes wherein the development of a specific fractal pattern occurred in discrete stages. The triangular pattern (see Fig. 1) coded by sites 1,2,3 was defined as stage I, that coded by the sites $1,\ldots,15$ was denoted stage II, that coded by $1,\ldots,42$ as stage III, and that coded by $1,\ldots,123$ as stage IV. We then assumed that the onset of growth at each stage required a chemically specific "trigger mechanism." In particular, we considered a molecule localized initially at site 1 which, upon activation, is released from site 1 and migrates randomly throughout the lattice, reacting eventually (and irreversibly) at a single, specific site (reaction center) on the far boundary of the system: For stages I–IV, the set of boundary sites is the one-dimensional sequence of points 2,3; 11,12,13,14; $34,\ldots,42$; and $107,\ldots,123$, respectively. Thus, suppose the pattern defined by stage II has been generated; in our model, once the diffusing coreactant reacts with the target molecule at a given reaction center on the boundary, we suppose that the nearest-neighbor information coded by rule 90 is processed at each of the points defining the boundary (i.e., the points $11,\ldots,14$) and the next stage (III) in the development of the pattern takes place.

The basic strategy taken in our earlier work was to calculate, using the theory of finite Markov processes, the first moment of the probability distribution function describing the above pattern generation process (specifically, the mean walk length of the coreactant diffusing from site 1 to a target site). The consequences of considering several possible locations of the reaction center were examined and the whole calculational procedure carried through both for the Sierpinski gasket (diagrammed in Fig. 1) and for the associated, triangular (Euclidean) lattice (e.g., for $N=15$, the structure diagrammed in Fig. 1 with all sites $1,\ldots,15$ connected). Upon examining the values of the mean walk length of the coreactant diffusing from site 1 ($\langle n\rangle_1$) (as well as the overall average walk length $\langle n\rangle$) to target molecules similarly positioned on the two lattice structures considered, we inferred that the development of fractal patterns is distinctly slower than for regular (Euclidean) ones.

As recognized in our earlier study, the conclusion

 

drawn from calculations of the stochastic variable $\langle n \rangle_1$ (or $\langle n \rangle$) can be made more precise by studying explicitly the full dynamics of the process (rather than inferring the dynamics from calculations of the mean walk length and estimates of the mean jump time between adjacent lattice points). To this end we have taken up in this paper the formulation and (numerical) solution of the (time-dependent) stochastic master equation for the model described above. Determination of the zero-mode relaxation time for the process considered and extraction of an effective relaxation time descriptive of the overall decay of the initial state of the system allow a more definite statement to be made regarding the unfolding of (representative) fractal or Euclidean patterns triggered by a site-specific recognition event (or reactive process).

The formation of the stochastic master equation and analysis of the attendant eigenvalue spectrum for the model are presented in Sec. II. In Sec. III we display graphically some of the principal trends uncovered in our study. Finally, in Sec. IV after summarizing the overall conclusions that can be drawn from the calculations reported here, we speculate on the possible relevance of these results to a concrete problem in biophysics. An issue which is of much interest today in experimental studies of neural networks is the manner in which patterns of neuronal connections are generated. The model elaborated here (which, in fact, was designed with this problem in mind) allows some preliminary conclusions to be drawn regarding the extent to which the neural network itself influences ("participates in") its further growth.

## II. THE STOCHASTIC MASTER EQUATION

The time dependence of diffusion-controlled reactive processes can be studied by formulating a stochastic master equation

$$\frac{d\rho_i}{dt} = -\sum_{j=1}^{N} G_{ij}\rho_j(t) \quad (i=1,2,\ldots,N) \tag{1}$$

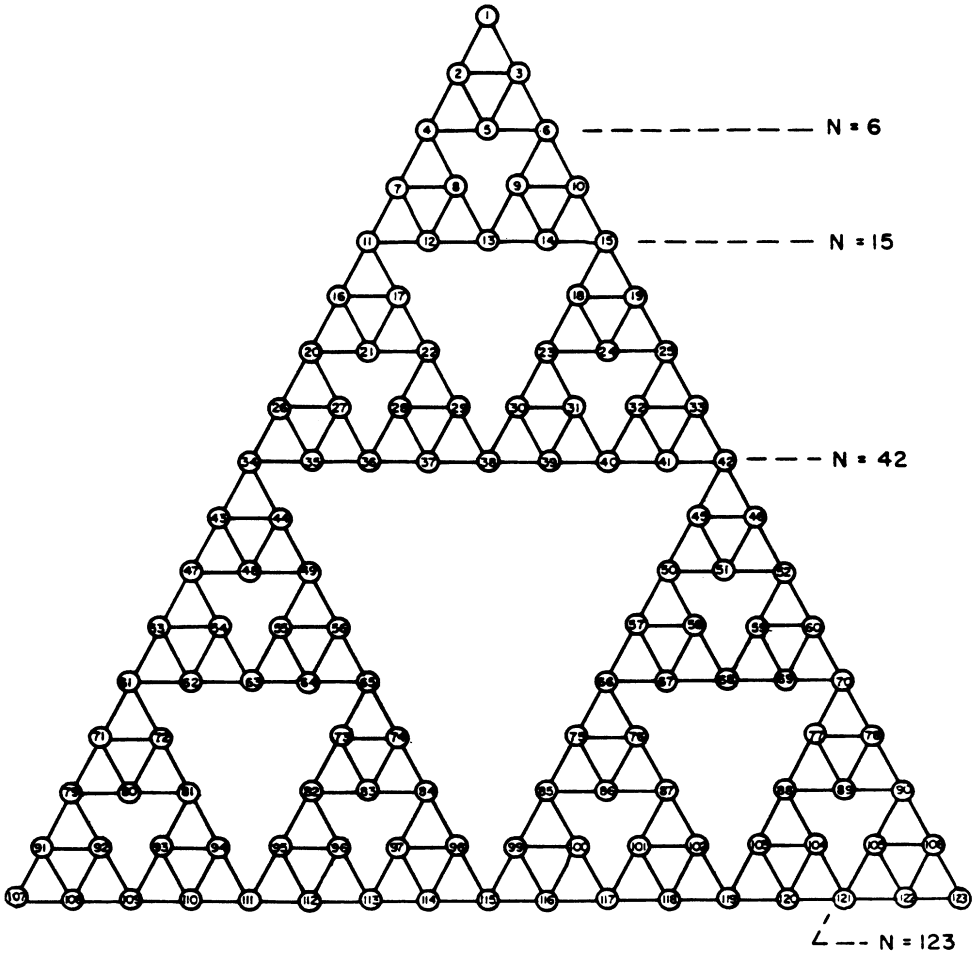


FIG. 1. The Sierpinski gasket with sites coded.

for the specific geometry characterizing the reaction space of the system. Here $\rho_i(t)$ is the probability of realizing a particular state $i$ and $G_{ij}$ is an $N \times N$ matrix that describes the transition probabilities between the states of the system. As is demonstrated in Refs. 2, 6, and 7, the general solution of the above system of linear equations is of the form

$$\rho_i(t) = \sum_{m=1}^{N} a_{im} e^{-\lambda_m t}, \tag{2}$$

where $a_{im}$ are coefficients determined by the initial conditions and $\lambda_m$ are the eigenvalues of the $G$ matrix above.

Two classes of initial conditions are considered in this study and these will now be described. Consider first a coreactant initiating its motion at the (top) vertex site $k$ $(=1)$ of the lattice unit. From that moment $(t=0)$ on, the coreactant is assumed to diffuse randomly on the lattice from site to site until it reacts irreversibly with a target molecule anchored at a particular site on the far boundary (the base). The number of discrete steps in this trajectory will be some number, say $k_1$. Note, however, that the trajectory followed by the diffusing coreactant starting from that initial site $k$ is not unique; a variety of possible paths on the lattice can be taken by the coreactant and each will be characterized by a walk length $k_i$. The most probable or average walk length will be the statistical average of all possible paths from site $k$ to the reaction center and this number will be denoted $\langle n \rangle_k$. Of course, one could imagine the coreactant starting its trajectory at any one of the $N-1$ satellite sites defining the lattice under study. The corresponding, overall average walk length characterizing all possible flows from all possible nontrapping sites will be denoted $\langle n \rangle$.

Relative to the system of Eqs. (1), the first class of initial conditions is specified by assigning $\rho_k(t=0)=1$ with $\rho_i(t=0)=0$ for all $i \neq k$. The second class of conditions is characterized by assigning $\rho_k(t=0) = (N-1)^{-1}$ for all $k$ (excluding the target site or trap).

For a given choice of initial condition, we consider systematically the unfolding of regular (triangular) or fractal (Sierpinski) patterns as triggered by site-specific reactive processes. In this work, the consequences of positioning the target molecule at two different locations are examined in detail. The first site, labeled $A$, is one of the (two) vertex sites on the "base" of the lattice structure extant at each generation; the second, labeled $B$, is the midpoint of the base at each generation of growth.

In studying the dynamics on the lattice structures considered here, it is important to note that the flow of the diffusing coreactant is constrained by the boundaries of the structure present at a given generation of growth. Thus we assume that when the diffusing coreactant is on a boundary site, only adjacent sites on the boundary or (nearest-neighbor) sites in the interior of the lattice are accessible to the coreactant. This constraint necessitates a distinction between the local versus global connectivity (or valency) of the lattice structure. Specifically, one must distinguish between the number $\nu_k$ of pathways (to or from) a particular lattice site $k$ versus the overall (or average) connectivity $\bar{\nu}$ of the lattice. For example, at each stage of generation, the Sierpinski gasket will have three vertex points characterized by a valency $\nu_k = 2$ while *all* other boundary and interior sites of the gasket will have a local valency $\nu_k = 4$. Thus the overall connectivity $\bar{\nu}$ of the network will change with each successive generation of growth as the number of interior and nonvertex boundary sites begins to dominate the number of vertex sites. In particular, for the Sierpinski gasket the overall (or average) valency $\bar{\nu}$ of the network changes systematically from $\bar{\nu}=3.600$ to 3.8571 to 3.9512 as $N$ changes from $N=15$ to 42 to 123. On the other hand,

TABLE I. Correspondence between $\langle n \rangle$, $\nu\lambda_1^{-1}$, and $\bar{\nu}\bar{\lambda}_1^{-1}$. SG denotes Sierpinski gasket.

| Pattern | $N$ | $T$ | $\bar{\nu}$ | $\langle n \rangle$ | $\lambda_1$ | $\bar{\nu}\lambda_1^{-1}$ | $D_1(\%)$[a] | $\bar{\lambda}$ | $\bar{\nu}\bar{\lambda}^{-1}$ | $D_2(\%)$[b] |
|---|---|---|---|---|---|---|---|---|---|---|
| Triangle or SG | 3 | $A$ | 2.0000 | 2.0000 | 1.000 000 | 2.000 | 0.00 | | | |
| Triangle | 6 | $A$ | 3.0000 | 9.200 | 0.330 921 | 9.066 | −1.46 | | | |
| or SG | | $B$ | 3.0000 | 3.800 | 0.697 224 | 4.303 | 13.24 | | | |
| Sierpinski | 15 | $A$ | 3.6000 | 43.429 | 0.080 844 3 | 44.530 | 2.54 | 0.081 628 6 | 44.102 | 1.55 |
| | | $B$ | 3.6000 | 17.714 | 0.183 897 | 19.576 | 10.51 | 0.186 602 | 19.292 | 8.91 |
| Triangle | 15 | $A$ | 4.0000 | 44.674 | 0.089 145 7 | 44.870 | 0.44 | 0.090 380 6 | 44.257 | −0.93 |
| | | $B$ | 4.0000 | 17.723 | 0.212 013 | 18.867 | 6.45 | 0.212 672 | 18.808 | 6.12 |
| Sierpinski | 42 | $A$ | 3.8571 | 211.561 | 0.017 327 3 | 222.602 | 5.22 | 0.019 463 2 | 198.174 | −6.33 |
| | | $B$ | 3.8571 | 85.342 | 0.040 340 2 | 95.614 | 12.04 | 0.045 254 9 | 85.231 | −0.13 |
| Triangle | 45 | $A$ | 4.8000 | 223.809 | 0.021 147 9 | 226.973 | 1.41 | 0.021 871 5 | 219.464 | −1.94 |
| | | $B$ | 4.8000 | 85.284 | 0.054 087 1 | 88.745 | 4.06 | 0.055 255 3 | 86.869 | 1.86 |
| Sierpinski | 123 | $A$ | 3.9512 | 1047.312 | 0.003 546 48 | 1114.118 | 6.38 | 0.003 579 30 | 1103.903 | 5.40 |
| | | $B$ | 3.9512 | 420.262 | 0.008 314 27 | 475.231 | 13.08 | 0.008 407 48 | 469.962 | 11.83 |
| Triangle | 153 | $A$ | 5.3333 | 1118.42 | 0.004 700 17 | 1134.710 | 1.46 | 0.004 711 14 | 1132.068 | 1.22 |
| | | $B$ | 5.3333 | 437.95 | 0.012 544 2 | 425.163 | −2.92 | 0.011 891 9 | 448.485 | 2.41 |

[a] $D_1(\%) = [(\bar{\nu}\lambda_1^{-1} - \langle n \rangle)/\langle n \rangle] \times 100$.
[b] $D_2(\%) = [(\bar{\nu}\bar{\lambda}^{-1} - \langle n \rangle)/\langle n \rangle] \times 100$.

the triangular lattice will be characterized by three different local valencies $\nu_k$. As for the Sierpinski gasket, the vertex sites will be characterized by $\nu_k=2$ and the boundary sites by $\nu_k=4$ but all interior sites of the triangular lattice will be characterized by a local valency $\nu_k=6$. Thus the global (or average) valency $\bar{\nu}$ of the triangular lattice changes systematically in successive generations from $\bar{\nu}=4.000$ to 4.800 to 5.333 as $N$ changes from $N=15$ to 45 to 153.

The eigenvalue spectrum $\{\lambda_m\}$ has been determined at each generation of growth both for the regular (triangular) pattern (lattices $N=6$, 15, 45, and 153) and the fractal (Sierpinski) pattern (lattices $N=6$, 15, 42, and 123), for both choices of initial conditions. One can prove that, for $N$ large, the reciprocal of the smallest eigenvalue $\lambda_1$ of the $G$ matrix (the zero-mode relaxation time) is related to the first moment (the mean walk length $\langle n \rangle$) of the underlying probability distribution function governing the process.[2,6,7] The formal relationship is

$$\langle n \rangle = \nu \lambda_1^{-1} \tag{3}$$

so that the correspondence involves the valency $\nu$ of the surface considered.

The extent to which the single eigenvalue $\lambda_1$ dominates the decay can be gauged by fitting the overall evolution curves (see, e.g., the profiles displayed in Sec. III) to a two-term polynomial of the form $\ln\rho(t)=\ln\bar{a}-\bar{\lambda}t$, and determining $\bar{\lambda}$ via a least-squares procedure. The $\bar{\lambda}$ encompasses information on the set $\{\lambda_m\}$ for each lattice structure considered. Documented in Table I are values of $\lambda_1$ and $\bar{\lambda}$ for that choice of initial condition wherein the diffusing coreactant may start its migration from any (nontrapping) site with equal *a priori* probability. The close correspondence between $\lambda_1$ and $\bar{\lambda}$ shows clearly the dominance of the eigenvalue $\lambda_1$ in driving the decay of the system of Eqs. (1). Also listed in Table I are the quantities $\bar{\nu}\lambda_1^{-1}$ and $\bar{\nu}\bar{\lambda}^{-1}$ together with the (previously reported) values of $\langle n \rangle$ for this choice of initial condition, so that an assessment of the correspondence (3) noted above can also be made.

From these calculations, two general features emerge: (1) the correspondence [Eq. (3)] between the random-walk characteristic $\langle n \rangle$ and the dynamical parameter $\lambda_1^{-1}$ is good for most of the cases examined and, (2) the decays on all lattice units studied are effectively dominated by the single eigenvalue $\lambda_1$. It is evident from the structure of the formal solution (2) to the system (1) that $\lambda_1$ may be interpreted as an effective first-order rate constant (or $\lambda_1^{-1}$ as characteristic relaxation time) of the system.

## III. RESULTS

We consider first the survival probability $\rho(t)$ of a coreactant diffusing on an $N=6$ triangular lattice with a single reaction center (target molecule) anchored at one of the vertex sites ($A$) on the base versus the case where the target molecule is localized at the midpoint ($B$) of the base. Both for the case where one assumes an equal *a priori* probability of the diffusing coreactant being at any of the $N-1$ satellite sites at time $t=0$ (Fig. 2) and the case where the diffusing coreactant is assumed to initiate its motion at the vertex site farthest removed from the base (Fig. 3), one finds that the coreactant survives longer when the target molecule is at a base vertex position.

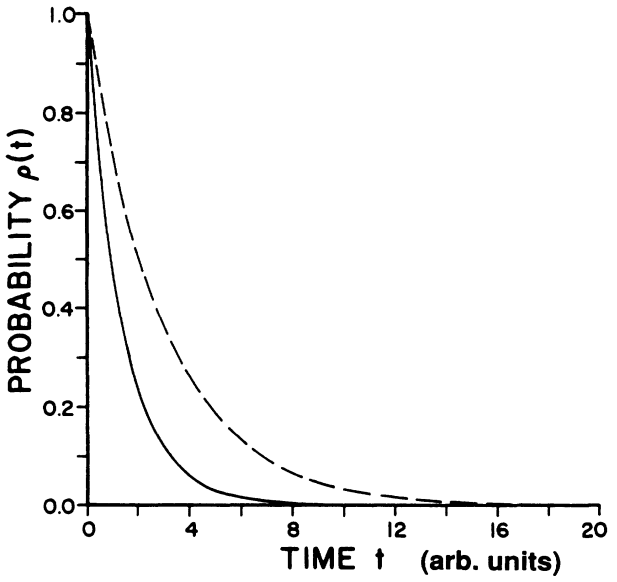


FIG. 2. The survival probability $\rho(t)$ of a coreactant diffusing on an $N=6$ triangular lattice with a single reaction center (target molecule) anchored at one of the vertex sites on the base (dashed line) or at the midpoint of the base (solid line). As the initial condition we assume an equal *a priori* probability of the diffusing coreactant being at any of the $N-1$ satellite sites at time $t=0$.

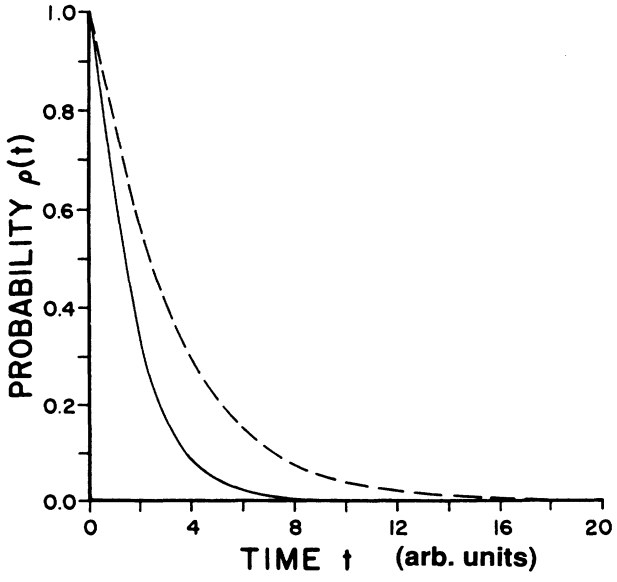


FIG. 3. The conventions here are the same as in Fig. 2 except that we assume the diffusing coreactant initiates its motion at the vertex site farthest removed from the target on the base.

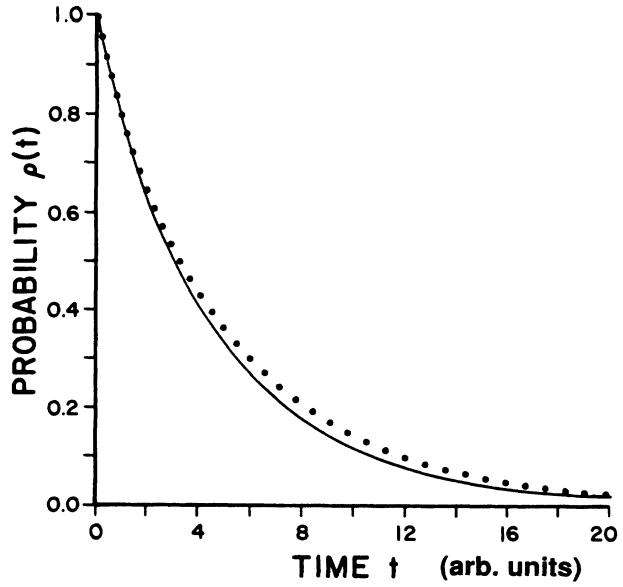


FIG. 4. The survival probability $\rho(t)$ of a coreactant diffusing on an $N=15$ triangular lattice (solid line) vs an $N=15$ Sierpinski gasket (dotted line). The target molecule is positioned at the midpoint of the base and, as the initial condition, we assume an equal *a priori* probability of the diffusing coreactant being at any of the $N-1$ satellite sites at time $t=0$.

This general conclusion pertains to all the lattices considered in this paper: the coreactant "finds" the target molecule much more easily when the latter is positioned at the centrosymmetric site on the base of the lattice unit.

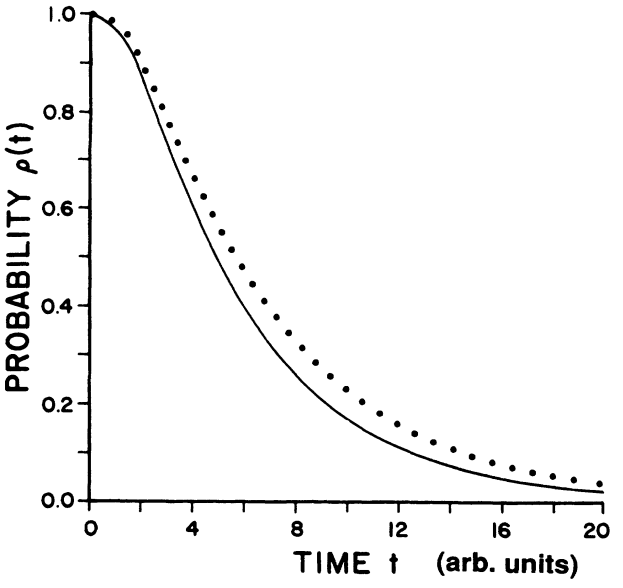


FIG. 5. The conventions here are the same as in Fig. 4 except that we assume the diffusing coreactant initiates its motion at the vertex site farthest removed from the target on the base.

The case $N=15$ is particularly interesting since this is the only (nontrivial) lattice unit for which a triangular lattice and a Sierpinski gasket have exactly the same number $N$ of total sites. In terms of bond connectivity (reaction pathways), however, the overall (effective) valence of the triangular lattice is $\bar{v}=4.000$ whereas that for the Sierpinski gasket is $\bar{v}=3.600$. In Figs. 4 and 5 we assume that the target molecule is anchored at the midpoint ($B$) of the base and find that, both for the case where the diffusing coreactant initiates its motion from any of the $N-1$ satellite sites with equal *a priori* probability (Fig. 4) or where the trajectory is initiated from the (top) vertex site farthest removed from the target (Fig. 5), decay on the fractal lattice is distinctly *slower* than on the regular lattice. These trends persist when one switches the target molecule to one of the vertex positions on the base (Figs. 6 and 7).

The next generation of the lattice structures results in an $N=42$ Sierpinski gasket and an $N=45$ triangular lattice. Despite the fact that the triangular lattice has three more satellite sites than the Sierpinski gasket, the trends noted in the preceding paragraph are still sustained: For both choices of initial condition, the decay on the fractal lattice is distinctly slower than on the regular lattice, regardless of whether the reaction center is positioned at the midpoint ($B$) of the base (Figs. 8 and 9) or at one of the vertex sites (Figs. 10 and 11).

The above conclusions may be brought out in a different way by comparing corresponding values of $\lambda_1$ for the Sierpinski gasket versus the triangular lattice as

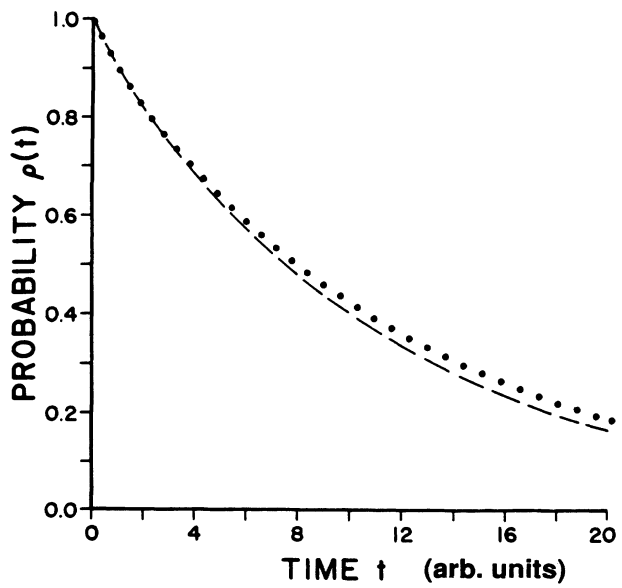


FIG. 6. The survival probability $\rho(t)$ of a coreactant diffusing on an $N=15$ triangular lattice (dashed line) vs an $N=15$ Sierpinski gasket (dotted line). The target molecule is positioned at one of the vertex sites on the base and, as the initial condition, we assume an equal *a priori* probability of the diffusing coreactant being at any of the $N-1$ satellite sites at time $t=0$.

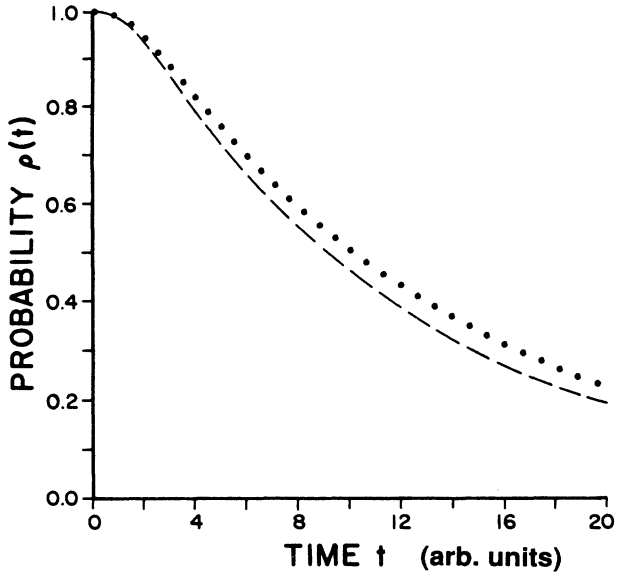


FIG. 7. The conventions here are the same as in Fig. 6 except that we assume the diffusing coreactant initiates its motion at the vertex site farthest removed from the base.

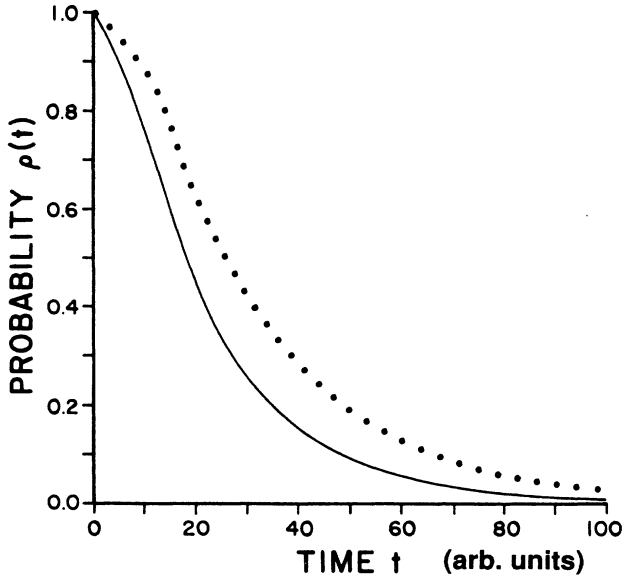


FIG. 9. The survival probability $\rho(t)$ of a coreactant diffusing on an $N=45$ triangular lattice (solid line) vs an $N=42$ Sierpinski gasket (dotted line). The conventions here are the same as in Fig. 5.

reported in Table I. The initial conditions relevant for the data specified in Table I are those for which the diffusing coreactant is assumed to initiate its trajectory from any of the $N-1$ satellite sites. As noted previously, $\lambda_1$ is the smallest eigenvalue of the system (1) and is the eigenvalue which dominates the decay of this initial state in the limit of long $t$. For every generation of lattice structure (i.e., $N=15,42,123$ for the Sierpinski gasket and $N=15,45,153$ for the triangular lattice) and for either location of reaction center [base midpoint ($B$) or vertex ($A$) site], it is seen that $\lambda_1$ for the triangular lattice is larger than the $\lambda_1$ for the Sierpinski gasket, even when a

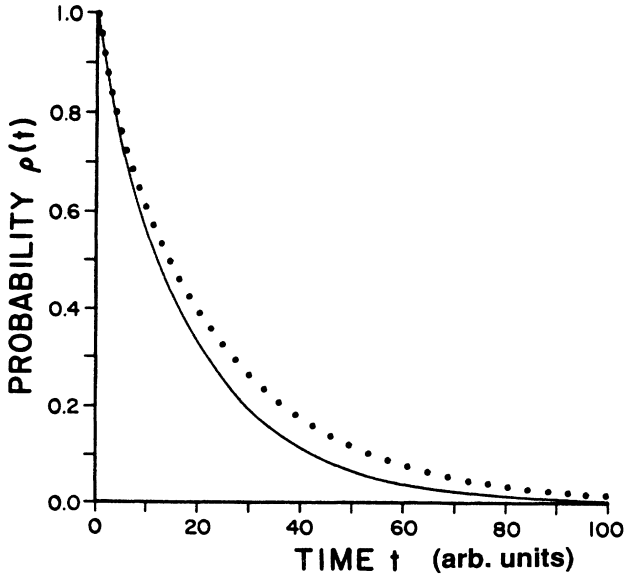


FIG. 8. The survival probability $\rho(t)$ of a coreactant diffusing on an $N=45$ triangular lattice (solid line) vs an $N=42$ Sierpinski gasket (dotted line). The conventions here are the same as in Fig. 4.

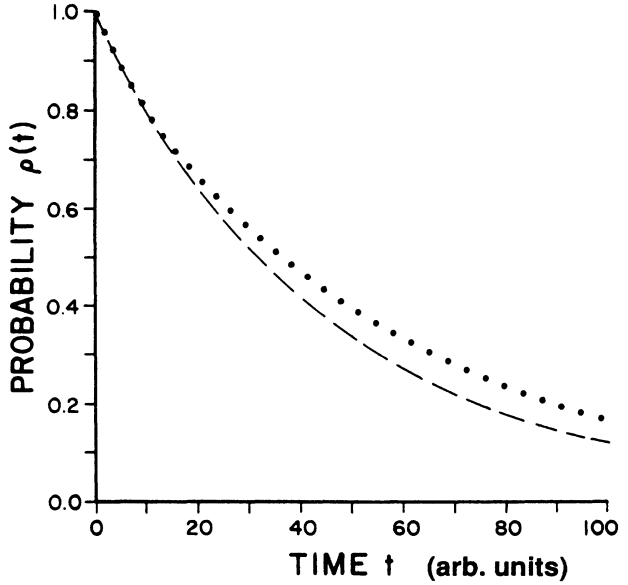


FIG. 10. The survival probability $\rho(t)$ of a coreactant diffusing on an $N=45$ triangular lattice (dashed line) vs an $N=42$ Sierpinski gasket (dotted line). The conventions here are the same as in Fig. 6.

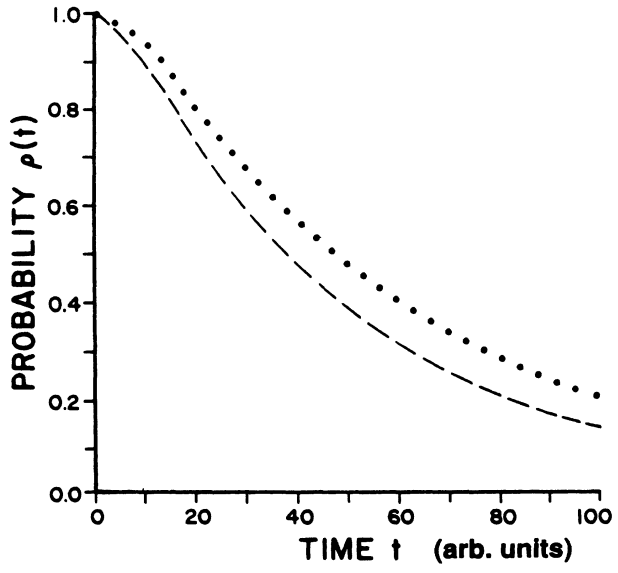


FIG. 11. The survival probability $\rho(t)$ of a coreactant diffusing on an $N=45$ triangular lattice (dashed line) vs an $N=42$ Sierpinski gasket (dotted line). The conventions here are the same as in Fig. 7.

given generation is characterized by a different number $(N-1)$ of satellite sites. Thus in stage IV of the pattern generation process, there are 30 more sites accessible to the diffusing coreactant on the triangular lattice $(N=153)$ than on the Sierpinski gasket $(N=123)$, yet the $\lambda_1$ value (and hence the decay rate) for the triangular lattice is $\sim 25\%$ larger than the $\lambda_1$ value for the Sierpinski gasket for a target molecule positioned at site $B$ (and $\sim 34\%$ larger for a target at site $A$). This result provides an important clue in understanding the importance of lattice connectivity in influencing the dynamics on the structures considered, a point which will be taken up in the following section.

## IV. CONCLUSIONS

The overall conclusion which follows from the calculations reported in this paper is that pattern development triggered by a site-specific recognition event (or reaction) on a Sierpinski gasket is distinctly slower than the corresponding process on a regular triangular structure. These results are entirely consistent with the theoretical predictions of Gefen, Aharony, and Alexander,[1] reported in their analytical study of diffusion on percolation versus Euclidean networks. They are also consistent with our earlier calculations[3] of the mean walk length $\langle n \rangle_1$ (or $\langle n \rangle$) for the model considered here. That the latter calculations are consistent with the present study follows from the large $N$ correspondence noted previously, viz., $\bar{\nu}\lambda_1^{-1}=\langle n \rangle$, where $\lambda_1$ is the smallest eigenvalue of the system (1). Generally speaking, this correspondence is quite close and, in fact, becomes even closer if one computes $\langle n \rangle$ using the average $\bar{\lambda}$. Recall that the latter quantity is an effective or overall calibration of the decay [constructed by performing a least-squares analysis of the data generated via numerical solution of the system (1)]. Thus $\bar{\lambda}$ gives an estimate of the influence of the complete set $\{\lambda_i\}$ of eigenvalues governing the decay or, conversely, gives a numerical estimate of the extent to which the overall decay is driven by the single eigenvalue $\lambda_1$ (the reciprocal of the zero-mode relaxation time). Since the correspondence between $\langle n \rangle$ and $\bar{\nu}\lambda_1^{-1}$ [or $\bar{\nu}\bar{\lambda}^{-1}$] is evidently quite good, one can use either characteristic, $\langle n \rangle$ or $\lambda_1$, to discuss the fate of a randomly diffusing coreactant on lattices of integral or fractal dimensions.

A second conclusion which follows from the work presented in this paper is that if the reaction center is positioned at a more centrally located site (the midpoint site $B$ versus the vertex site $A$) the efficiency of the diffusion-controlled reactive process is enhanced, regardless of the integral or fractal character of the lattice. Using the $\langle n \rangle$ values reported in Table I for targets positioned at site $B$ versus site $A$ to compute the percentage difference $D(\%)\equiv(\langle n \rangle_A-\langle n \rangle_B)/\langle n \rangle_A\times 100$, for the specific lattice considered, the difference is 59.2%, 59.7%, and 59.9% for the three, stages II–IV, in the unfolding of the Sierpinski gasket and 60.3%, 61.9%, and 60.8% for the same three stages in the growth of the triangular pattern. These results are fully in accord with one's intuition regarding the relative probability of encounter of the diffusing coreactant with a target positioned at site $B$ versus site $A$, but the near constancy of the percent difference in $\langle n \rangle$ ($\sim 60\%$) for *both* fractal and Euclidean patterns provides a useful benchmark in quantifying differences in reaction efficiency for the encounter-controlled process studied here.

It will be a principal aim of our subsequent work to make definite the relationship between our results and earlier theoretical work dealing with diffusion on fractals [see especially the recent review of Orbach,[8] the paper of O'Shaughnessy and Procaccia[9] (and references cited therein), and the work of Blumen *et al.*[10] and others[11]]. In a somewhat broader context, it is interesting to compare the structure of the evolution curves [i.e., $\rho(t)$ versus $t$] generated for the two choices of initial condition considered here in the neighborhood of $t=0$. In more descriptive language, the initial condition $\rho_k(t=0)=1$ with $\rho_i(t=0)=0$ for all $i\neq k$ corresponds to evolution from a "pure state" while the second class, $\rho_k(t=0)=(N-1)^{-1}$ for all $k$, corresponds to evolution from a "manifold of states." The "shoulder" in the decay curve which appears when the former class of initial conditions is considered (compare Figs. 8 and 9, and Figs. 10 and 11) is reminiscent of the shoulder which appears when evolution from a pure state is studied in exactly solved Hamiltonian models. This effect, noticed by Zwanzig[12] nearly 30 years ago in his study of the master equation and of the statistical mechanics of irreversibility, was corroborated in a study of the exact dynamics of an excited two-level atom in a radiation field;[13] in the latter study, based on the quantum-mechanical master equation, the pure state from which evolution occurred was a single level of the excited atomic system. In the present study (based on a stochastic master equation), the pure state is the (top) vertex site $k=1$ (see Fig. 1).

There are two senses in which differences in the time scale (or the $\langle n \rangle_1$ or $\langle n \rangle$ values) characterizing the decay of the initial state (for either choice of initial condition) on fractal versus Euclidean lattices may be attributed to differences in the topological structure of the underlying lattice. The first is that which is captured in the seminal work of Mandelbrot[5] and the research reported in Refs. 1 and 8–11, i.e., the concept of *fractal* dimensionality. A different perspective can be provided by taking advantage of results obtained in studying the dependence on lattice valency of random walks on lattices of *integral* dimensionality. In a recent study[14] of random walks on $d=2$ finite lattices subject to confining (or periodic) boundary conditions with a centrally located (deep) trap, calculated values of $\langle n \rangle$ were compared with those predicted using analytic (asymptotic) expressions derived by Montroll[15] (and revised by den Hollander and Kasteleyn[16] for square planar lattices). Specifically, results calculated for $d=2$ lattices of valency $v=3$, 4, and 6 reconfirmed the essential correctness of Montroll's asymptotic results in the limit of large $N$. The leading term in the Montroll expressions is of the form

$$\langle n \rangle \sim \frac{N}{N-1}(A_1 N \ln N) , \tag{4}$$

with

$$A_1=\frac{3\sqrt{3}}{4\pi}=0.413\,496\,672 \quad \text{for } v=3 ,$$

$$A_1=\frac{1}{\pi}=0.318\,309\,886 \quad \text{for } v=4 ,$$

$$A_1=\frac{\sqrt{3}}{2\pi}=0.275\,664\,448 \quad \text{for } v=6 .$$

Thus, it may be seen that for a given $N$ and a common metric, the value of $\langle n \rangle$ calculated for a $d=2$ Euclidean lattice *decreases* with an *increase* in the valency characterizing the underlying lattice. Let us now examine the relevance of this insight to results reported in the present study. As noted previously, the effective or overall valency $\bar{v}$ of the Sierpinski gasket converges to $\bar{v}=4$ with increase in $N$ while the $\bar{v}$ for the triangular lattice unit converges to $\bar{v}=6$; given Montroll's results, we anticipate that for lattices characterized by a common value of $N$, $\langle n \rangle$ should be smaller on lattices of valency $\bar{v}=6$ than on lattices of valency $\bar{v}=4$ in the limit of large $N$. A plot of $\langle n \rangle$ versus $N$ using the data presented in Table I (see also Figs. 2 and 3 in Ref. 3) confirms this expectation for $N>15$. This ordering can also be inferred by comparing the ratio

$$\frac{\langle n \rangle_{\text{Sier, } N=123}}{\langle n \rangle_{\text{tri, } N=153}}=\frac{1047.312}{1118.42}=0.936 , \tag{5}$$

calculated using the data presented in Table I, with the value calculated using Eqs. (4), namely,

$$\frac{\langle n \rangle_{\text{Sier, } N=123}}{\langle n \rangle_{\text{tri, } N=153}} \sim \frac{\left[\frac{N}{N-1}A_1 N \ln N\right]_{N=123,\bar{v}\sim 4}}{\left[\frac{N}{N-1}A_1 N \ln N\right]_{N=153,\bar{v}\sim 6}}=0.889 ,$$

a difference of 5.0% vis-à-vis the result (5). [Use of the full (four-term) asymptotic expression for $\langle n \rangle$ for each valency (see Table VII of Ref. 14) yields a percent difference of 8.4%.] The closeness of these results (despite the somewhat different boundary conditions) suggests that it may be useful in some applications to regard flows on lattices of *fractal* dimensionality as flows on lattices of *integral* dimensionality (here, $d=2$) but of "fractal" valency.

Finally, it is of interest to speculate on the possible relevance of results obtained in the present work to a concrete physical problem and to this end we focus on an issue which is of much interest today in experimental studies of neural networks, specifically the generation of patterns of neuronal connections. Until relatively recently, the standard view (the "chemoaffinity theory") has been that these connections are the consequence of (unique) complementary recognition molecules on the pre- and postsynaptic cells. Over the last decade, however, experiments have tended to suggest that specific connections (in vertebrates) probably involve (1) competition between axon terminals, (2) trophic feedback between pre- and postsynaptic cells, and (3) modifications of connections by functional activity.[17] Thus the difference between these two views relates to the extent of participation of the neural network itself in influencing its further growth.

The type of (vertebrate) neuronal network to which our study might apply is the cerebellar Purkinje cell. This cell represents an extreme in neuronal specialization, as may be appreciated by examining illustrations in standard texts.[18] Despite its complexity, however, the extensive dendritic arborization of the Purkinje cell is not bushlike but rather planar. It is known that signal transmission in this network is initiated via interaction (synapse) with millions of axons which pass through the holelike spaces in the dense arborization; in the language of Hubel,[18] these axons run "like telephone wires perpendicular to the plane" of the Purkinje network.

The fractal and Euclidean patterns studied here represent two idealizations of Purkinje dendritic structure. The sites $A$ and $B$ on the frontier of these fractal or Euclidean patterns may be regarded as sites at which a recognition event can occur. The issue then is whether the many axons which play a role in signal transmission once the dendritic network is fully developed also play a role in "guiding" pattern development at an earlier stage of morphogenesis. Calculations on our model suggest that regardless of the pattern generated (fractal or Euclidean), activation of the developing network at a manifold of sites rather than a stimulus propagated from a somatic source (here, the site $k=1$) leads to an accelerated unfolding of subsequent stages in the pattern (compare Figs. 2 and 3, 4 and 5, 6 and 7, 8 and 9, and 10 and 11).

The above ordering can be seen in a more direct way by comparing the $\langle n \rangle_1$ versus $\langle n \rangle$ values reported in Ref. 3, from which one finds that $\langle n \rangle_1 > \langle n \rangle$ for all $N$. Moreover, using these data, an interesting difference emerges in studying the development of the Sierpinski gasket versus the triangular lattice. If one computes the percent difference, $D(\%)\equiv[(\langle n \rangle_1-\langle n \rangle)/\langle n \rangle_1\times 100]$

for a target positioned at the frontier site $B$, one finds an *increase* from 29.1% to 31.7% to 32.7% for stages II–IV in the development of the Sierpinski gasket but a *decrease* from 23.7% to 21.7% to 18.2% for the triangular lattice. The corresponding percentages calculated for the frontier site $A$ are 13.1% (stage II), 15.4% (stage III), and 16.2% (stage IV) for the Sierpinski pattern and 11.1% (stage II), 10.8% (stage III), and 9.4% (stage IV) for the triangular one. These data clearly show that differences between single-site versus multiple-site activation of the network become of less consequence with growth of the regular (Euclidean) pattern but of somewhat greater consequence for the fractal one. Since the fractal pattern more nearly represents the complicated pattern structure of the Purkinje network, we conjecture that multiple-site (e.g., axonal) stimulation of the developing neuronal pattern is the more efficient morphogenetic process.

## ACKNOWLEDGMENTS

This work was initiated at the University of Notre Dame, Notre Dame, Indiana. The research was supported in part by the Office of Basic Energy Sciences of the Department of Energy.

*Author to whom correspondence should be addressed.

[1]Y. Gefen, A. Aharony, and S. Alexander, Phys. Rev. Lett. **50**, 77 (1983).

[2]H. Haken, *Synergetics, An Introduction,* 3rd ed. (Springer-Verlag, Berlin 1983); *Advanced Synergetics,* 2nd ed. (Springer-Verlag, Berlin 1987).

[3]G. D. Abowd, R. A. Garza-López, and J. J. Kozak, Phys. Lett. A **127**, 155 (1988).

[4]S. Wolfram, Rev. Mod. Phys. **55**, 601 (1983).

[5]B. B. Mandelbrot, *The Fractal Geometry of Nature* (Freeman, San Francisco, 1983).

[6]E. W. Montroll and K. E. Shuler, Adv. Chem. Phys. **1**, 361 (1958).

[7]G. Nicolis and I. Prigogine, *Self-Organization in Nonequilibrium Systems* (Wiley, New York, 1977).

[8]R. Orbach, Science **231**, 814 (1986).

[9]B. O'Shaughnessy and I. Procaccia, Phys. Rev. A **32**, 3073 (1985).

[10]A. Blumen, J. Klafter, and G. Zumofen, Phys. Rev. B **28**, 6112 (1983); A. Blumen, J. Klafter, B. S. White, and G. Zumofen, Phys. Rev. Lett. **53**, 1301 (1984).

[11]S. Alexander and R. Orbach, J. Phys. (Paris) Lett. **43**, L625 (1982); R. Rammal and G. Toulousse, *ibid.* **44**, L13 (1983).

[12]R. W. Zwanzig, in *Lectures in Theoretical Physics (Boulder, 1960),* edited by W. E. Brittin, B. W. Downs, and J. Downs (Interscience, New York, 1961).

[13]R. Davidson and J. J. Kozak, J. Math. Phys. **19**, 1074 (1978).

[14]P. A. Politowicz and J. J. Kozak, Langmuir **4**, 305 (1988).

[15]E. W. Montroll, J. Math. Phys. **10**, 753 (1969).

[16]W. Th. F. den Hollander and P. W. Kasteleyn, Physica A (Amsterdam) **112A**, 523 (1982).

[17]See the recent discussion by S. S. Easter, Jr., D. Purves, P. Rakic, and N. C. Spitzer, Science **230**, 507 (1985).

[18]D. H. Hubel, *Eye, Brain, and Vision* (Freeman, San Francisco, 1988).